Soil Microbes Transform Inorganic Carbon into Organic Carbon by Dark Fixation Pathways in Desert Soil

Zhen Liu[1,2], Yanfei Sun[1], Yuqing Zhang[1,3], Wei Feng[1,3], Zongrui Lai[1,3], Shugao Qin[1,4]

[1]Yanchi Research Station, School of Soil and Water Conservation, Beijing Forestry University, Beijing 100083, P. R. China

[2]Yellow River Delta Modern Agricultural Engineering Laboratory, Institute of Geographic Sciences and Natural Resources Research, Chinese Academy of Sciences

[3]Key Laboratory of State Forestry Administration on Soil and Water Conservation, Beijing Forestry University, Beijing 100083, P. R. China

[4]Engineering Research Centre of Forestry Ecological Engineering, Ministry of Education, Beijing Forestry University, Beijing 100083, P. R. China

Corresponding author: Yuqing Zhang (zhangyqbjfu@gmail.com)

Key Points:

- Soil inorganic carbon may be employed by certain microbes and transformed into organics; however, this remains largely unexplored.
- We performed *in situ* ^{13}C tracing in the desert soil and predict associated metabolisms by metagenomics.
- The study highlights a neglected carbon transformation process from inorganic to organic carbon mediated by soil microbes in drylands.

Abstract

Soil inorganic carbon (SIC) represents the main soil carbon pool in drylands with a high geologic residence time for carbon sequestration. Recent studies have shown that SIC is not stable as previously supposed, and can be employed by certain microbes and transformed into organics in soils; however, this transformation remains largely unexplored. We performed *in situ* ^{13}C tracing in desert bulk soil and employed metagenomics to predict the microbial metabolic processes associated with carbon transformation. The tracing data showed that the ^{13}C signature profile in soil organic carbon (SOC) originated from SIC with a ^{13}C-SOC content of 6.881 mg m^{-2} during the feeding periods. Metagenomic analysis identified genes encoding enzymes related to microbial CO_2 and HCO_3^- fixation, accounting for 0.448% (based on Kyoto Encyclopedia of Genes and Genomes database) and 0.668% (based on Evolutionary genealogy of genes: Non-supervised Orthologous Groups database) of all ascertained genes. Our results confirmed that a considerable portion of the determined genes and taxa were responsible for heterotrophic fixation. The microbes involved in dark microbial fixation, particularly chemoautotrophic and heterotrophic pathways, were from a broad taxonomic range. Although the amount of SOC derived from the dark microbial fixation process was not assessed, the present study highlights a neglected carbon transformation process mediated by soil microbes in drylands and provides insights into carbon transformation of SIC to SOC in dryland soil.

1. Introduction

Drylands are ecosystems that cover more than 40% of the terrestrial surface (Reynolds et al., 2007; Safriel & Adeel, 2005). These regions represent the major pool of soil inorganic carbon (SIC) and account for 15.5% of the world's soil organic carbon (SOC) storage (Lal, 2009), wherein the SIC pool is ten-fold higher than the SOC storage (Emmerich, 2003; Shi et al., 2012; Zamanian et al., 2016). Given that the carbon in SIC (85,000 years) has a longer mean residence time compared to SOC (35 years), vegetation (10 years), and atmosphere (5 years) (Monger et al., 2015), the dynamics of SIC in drylands may be of particular importance in the carbon cycles of terrestrial ecosystems, especially in the context of increased anthropogenic activity and global climate change (Gao et al., 2018; Zamanian et al., 2018). In addition, studies of soil organic matter in terms of formation, decomposition, transformation, and stabilization in drylands are relevant because of the mounting interest in investigating global carbon sequestration and soil nutrient condition in oligotrophic environments (Alonso-Sáez et al., 2010; Bay et al., 2018; Liang et al., 2017). Therefore, the dynamics and fate of the soil carbon pools in drylands are an essential and important topic of research.

A growing body of research reveals that carbon transformation processes occur between these two carbon pools (SOC and SIC), which is significant for understanding the formation, turnover, and stability of soil carbon pools in drylands (Liang et al., 2017; Liu et al., 2018 and 2020). Therein, soil microbes serve as a "microbial carbon pump" to regulate soil carbon dynamics via various metabolic pathways (Liang et al., 2017). In certain areas of drylands, SIC accumulation is

closely related to SOC accumulation following vegetation rehabilitation (Wang et al., 2015; Gao et al., 2018), which involves a carbon transformation process from SOC to SIC ("SOC→SIC"). In the process of "SOC→SIC," soil microbes are assumed to link the two carbon pools through the decomposition of organic matter and forming carbonates via certain metabolic pathways (Liu et al., 2018, 2020). As SIC mainly comprises of carbonates, followed by HCO_3^-, CO_3^{2-}, and CO_2 in drylands, recent studies associated with microbial carbon fixation, also hint at a carbon transformation process from SIC to SOC ("SIC→SOC") in the soil.

Recent studies have shown that autotrophic microbes in drylands contain the genetic potential for incorporating CO_2 and/or HCO_3^- into SOC, and are distributed in a range of natural surroundings, such as grasslands and semiarid deserts (Liu et al., 2018; Lynn et al., 2017; Zhao et al., 2018). The metabolic pathways involved in carbon transformation include both phototrophic and non-phototrophic processes via the operations of the Calvin cycle in the presence of light, and alternative chemoautotrophic pathways such as the reductive citrate cycle (rTCA cycle), hydroxypropionate-hydroxybutylate cycle (3-HP/4-HB cycle), dicarboxylate-hydroxybutyrate cycle (DC/4-HB cycle), 3-hydroxypropionate bi-cycle (3-HP cycle), and reductive acetyl-CoA pathway (WL pathway) (Alonso-Sáez et al., 2010; Bar-Even et al., 2012; Hügler & Sievert 2011; Liu et al., 2018). These pathways were identified based on the occurrence of genes involved in autotrophic pathways. Moreover, heterotrophic microbial CO_2 fixation for internal carbon cycling in the dark has been identified in arctic, cropland, temperate forest, and temperate soils (Miltner

et al., 2004; Nel & Cramer 2019; Šantrůčková et al., 2018; Spohn et al., 2020). This process may also contribute to the transformation of "SIC→SOC" in drylands; however, it remains largely unexplored in drylands. Taken together, we speculate the occurrence of a microbial transformation process from SIC to SOC in the soil of drylands; that is, soil microbes transform SIC, including soil CO_2 and/or HCO_3^-, into SOC pool via microbial fixation processes. Thus, microbial carbon transformation in drylands ("SIC→SOC") needs to be investigated, particularly the possibility of SIC (soil CO_2 and/or HCO_3^-) to be incorporated into SOC via microbial metabolic processes and the associated microbial pathways.

We hypothesized that SIC (soil CO_2 and/or HCO_3^-) can be transformed into SOC through dark reactions by microbes in the soil of drylands. Specifically, we expected to detect: (1) the signature of SIC, incorporated by microbial fixation processes, in the SOC; and (2) the related functional and taxonomic potential of soil microbial fixation and carbon transformation. To test the above hypotheses, we performed an *in situ* ^{13}C tracing experiment in bulk soil to track the fate of SIC in the Mu Us Desert of northern China. In addition, we used metagenomics to analyze the target genes and microbes that contribute to transforming soil CO_2 and HCO_3^- into SOC.

2. Materials and methods

2.1. Research site

We conducted this study on the south-western edge of the Mu Us Desert, China (37°42′N, 107°13′E; 1509 m above sea level). The study site is characterized by a

116 typical temperate continental climate, with a mean annual precipitation of 275 mm
117 and an annual potential evaporation of approximately 2014 mm. The mean annual
118 temperature is 7.60 °C and the frost-free period lasts approximately 128 d. The main
119 soil type is quartisamment (derived from Aeolian sand) with an electric conductivity
120 of 4.84 ds cm^{-1} and a pH of 8.90 (Liu et al., 2015, 2018). The 0-20 cm layer of the
121 main soil is composed of 97.04% sand, 11.56% silt, and 1.40% clay (Liu et al., 2020).
122 The SOC, SIC, and soil total nitrogen content at the research site are 3.65 g kg^{-1}, 3.78
123 g kg^{-1}, and 0.266 g kg^{-1}, respectively (Liu et al., 2015, 2018, 2020). Vegetation in the
124 research site is dominated by shrub species *Artemisia ordosica Krasch, Salix*
125 *psammophila* C. Wang & Chang Y. Yang, and *Hedysarum mongolicum* Turcz. The
126 grass species in the site include *Leymus secalinus* (Georgi) Tzvelev, *Agropyron*
127 *cristatum* (L.) Gaertn, and *Pennisetum centrasiaticum* Tzvel (Jia et al., 2018).
128

129 **2.2. Determination of soil inorganic carbon transformation to soil organic carbon**

130 An *in situ* ^{13}C tracing experiment was conducted to determine the process of carbon
131 transformation from SIC to SOC by microbial fixation in desert soil. Specifically, in
132 mid-August of 2016, nine 20 m × 20 m sites dominated by *A. ordosica*, *S.*
133 *psammophila*, and *L. secalinus* (Figure 1a), were selected as sampling plots within the
134 2 km × 2 km area. In each sampling plot, three parallel positions were randomly
135 selected (Figure1b) for the tracing experiment. Cylindrical iron chambers (20.2 cm
136 diameter, 100 cm high, and 0.1 cm thick, with a sealed top; Figure 1c and d) were
137 used for feeding $^{13}CO_2$ into the desert soil. The ^{13}C feeding protocols are described

below. Before feeding, the sealed soil collars were primarily set up to avoid leakage of $^{13}CO_2$ during the process. Specifically, at each position, two steel soil collars (20 cm diameter, 20 cm high, 0.1 cm thick) were inserted as paired collars into the soil 1 m from one another. Next, the collars containing intact soil were excavated, and their bottoms were sealed with steel sheets. The sealed collars were backfilled in their antecedent positions for a 2-d equilibration with the surroundings (Liu et al. 2015). Of the three inserted collar pairs in every plot, one collar in each pair was selected for $^{13}CO_2$ feeding, while the other was not and served as a control. Overall, six soil collars (three for feeding and the others as controls) were established at each plot (Figure 1b).

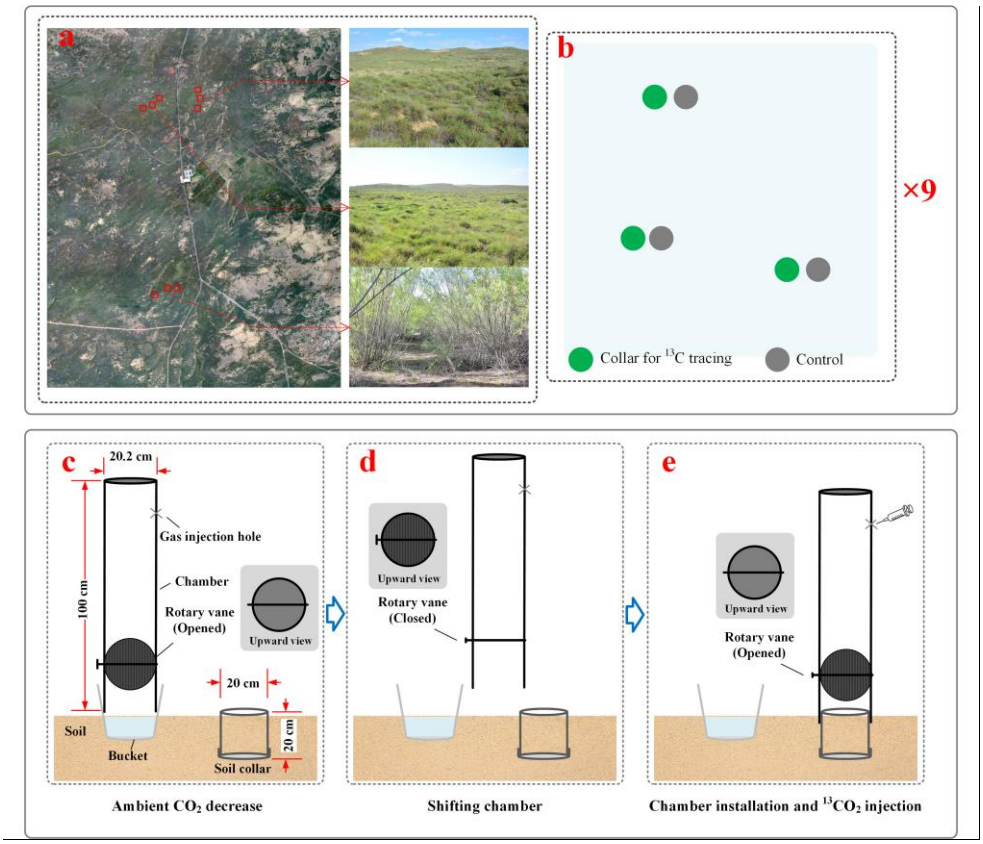

Figure 1. Selected typical sampling plots (a), parallel positions (b), and ^{13}C feeding protocols (c, d, and e) in the tracing experiment.

In each plot, three chambers were inserted into buckets containing 2 L of 6 M NaOH solution (Figure 1c) for 2 h with the rotary vane opened in order to decrease the ambient CO_2 in the chambers (from 400 to ~280 μmol mol^{-1}) and enhance the follow-up effectiveness of $^{13}CO_2$ feeding. Then, with the rotary vane closed (Figure 1d), the chambers were installed onto soil collars pushed 10 cm deep into the soil (Figure 1e). Next, 11.3 mL of $^{13}CO_2$ gas (concentration > 99.9%) was injected into the chamber via the gas injection hole (Figure 1e) to provide an initial $^{13}CO_2$ content of approximately 400 μmol mol^{-1}. Then, the rotary vane of the chamber was opened and the soil was exposed to $^{13}CO_2$ for 22 h. Equivalent feeding chambers with ambient CO_2 were installed on the remaining collars as control sets. Subsequently, 150 mL of gas in the chambers was extracted using an injection and used for ascertaining the CO_2 content and components ($^{12}CO_2$ and $^{13}CO_2$). Then, the chambers were moved away and their inner space was scoured by high-pressure gas to remove the remaining $^{13}CO_2$ and the CO_2 produced by soil respiration. In total, the feeding process was repeated once a day for 7 days. After feeding, 150 mL of the soil gaseous sample was extracted from each collar using a soil gas sampler (DIK-5520-13; Daiki Rika Kogyo, Saitama, Japan) and stored in aluminum foil bags to determine the soil CO_2 content and components. The CO_2 content and $\delta^{13}C$ of CO_2 of the obtained gas was analyzed using a Model CCIA-EPCO_2 isotope analyzer (912-0003; Los Gatos Research, Mountain View, CA, USA).

After performing the feeding protocols, 200 g of soil samples were collected from each collar using a soil auger. To determine the content of the microbial carbon transformation from SIC to SOC (^{13}C-SOC), 50 g of soil from each collar was air-dried and used for SOC and δ^{13}C analyses. The remaining fresh soil samples (150 g), collected from each collar in the same sampling plot, were mixed together in equal proportions to determine the soil bicarbonate content. The CO_2 content and δ^{13}C of the obtained soil gas were analyzed using a Model CCIA-EPCO_2 isotope analyzer (912-0003; Los Gatos Research, Mountain View, CA, USA). To determine the δ^{13}C of SOC, the air-dried sample was ground using an agate mortar, sieved through a 0.149 mm mesh, acidified using sulfurous acid (*v*:*w*, 4:100; Steinbeiss et al., 2008), and dried at 60°C prior to measurement. Then, the δ^{13}C was determined using an isotope ratio mass spectrometer (Thermo Finnigan Delta V; Thermo Fisher Scientific, Inc., Waltham, MA, USA). The reference substance utilized was Pee Dee Belemnite (R_{st} = 0.0112372). SOC was determined using the potassium dichromate oxidation method (Walkley & Black, 1934). Soil bicarbonate content was determined using the double-indicator neutral method (Wang et al., 2017).

2.3. Metagenomics prediction for microbial fixation

From each sampling plot, 12 soil cores were randomly obtained (depth range of 0–20 cm) using a sterilized soil auger (2.5 cm diameter), and thoroughly mixed as the representative sample. Before sampling, surface litter residues were removed. Each

composite sample was sieved through a 2 mm mesh to remove plant residues and roots, then stored at −78.5°C on dry ice for metagenomic analysis.

Total microbial DNA was isolated from 1.0 g of each soil sample using the MoBio Power soil DNA isolation kit (MoBio Laboratories, Carlsbad, CA, USA) following the manufacturer's instructions. The DNA sample was tested with regards to degradation degree and potential contamination, purity, and concentration. Then, 1 μg DNA per sample was used as input material for subsequent metagenomics sample preparation. Sequencing libraries were generated using the NEBNext® Ultra™ DNA Library Prep Kit for Illumina (New England BioLabs, Ipswich, MA, USA), and index codes were added to attribute sequences to each sample. Briefly, the DNA sample was fragmented by sonication to a size of 350 bp; then, DNA fragments were end-polished, A-tailed, and ligated with the full-length adaptor for Illumina sequencing with further polymerase chain reaction (PCR) amplification. Finally, PCR products were purified (AMPure XP system) and libraries were analyzed for size distribution using the Agilent 2100 Bioanalyzer (Agilent Technologies, Santa Clara, CA, USA) and quantified using real-time PCR. Clustering of the index-coded samples was performed using a cBot cluster generation system (TruSeq PE Cluster Kit v3-cBot-HS; Illumina, San Diego, USA). The prepared libraries were then sequenced using an Illumina HisSeq platform and paired-end reads were generated. The relative abundance of a gene was defined as the ratio of the sum of sequencing depth of every base in a predicted gene to gene length. To fully determine the functional groups associated with microbial fixation processes, metabolic pathway analyses were

performed using the Kyoto Encyclopedia of Genes and Genomes (KEGG; Kanehisa et al. 2004) and Evolutionary genealogy of genes: Non-supervised Orthologous Groups (eggNOG). BLASTP (e-value $\leq 1 \times 10^{-5}$) was used for amino acid alignments against the KEGG database (Version: 2015-12-04) and eggNOG database. The provided KEGG and eggNOG accession numbers denote the key enzymes used for annotation of the carbon transformation by microbial fixation (Table S1). Putative microbes were identified based on these KEGG accessions. Metagenomics data were submitted to NCBI under biosample accession number SAMN08366930.

2.4. Numerical and statistical analysis

The ratio of ^{13}C in SOC was calculated as follows:

$$AT = \frac{\left(1000 + \delta^{13}C\right) \times R_{st}}{1000 + \left(1000 + \delta^{13}C\right) \times R_{st}} \times 100 \quad (1)$$

Where, AT is the ratio of ^{13}C in SOC (%) and $\delta^{13}C$ is the isotopic signature of SOC.

The content of microbial transformation of inorganic to organic carbon (^{13}C-SOC) during the labeling periods was calculated as follows:

$$^{13}\text{C-SOC} = \frac{C_{SOC} \times B \times V \times (AT_{labelled} - AT_{control})}{S \times 100} \quad (2)$$

Where, ^{13}C-SOC is the content of the microbial carbon transformation from inorganic to organic (mg m^{-2}), C_{SOC} is SOC content (g kg^{-1}), B is soil bulk density (g cm^{-3}), V is soil volume in the soil collar (cm^3), S is the area of the soil collar (m^2), $AT_{labelled}$ is ratio of ^{13}C in SOC in the feeding set, and $AT_{control}$ is the ratio of ^{13}C in SOC in the control set.

The Mantel test was used to determine the correlation between the genes and composition of microbes facilitating inorganic carbon fixation and ^{13}C-SOC formation. Pearson's correlation analysis was conducted to analyze the relationship between ^{13}C-SOC and bicarbonate, CO_2, $^{13}CO_2$, and $^{12}CO_2$ content in the soil. Additionally, data on putative microorganisms encoding carbon fixation genes, identified at sample plots, were analyzed by principal component analysis (PCA) using the vegan package in R, with a linear regression analysis of PC1, PC2, or PC3 scores, and ^{13}C-SOC to analyze the relationship between the microbial community composition and microbial carbon transformation. Values were considered statistically significant at $P < 0.05$ and the marginal significance was defined as $0.05 < P < 0.10$. All statistical analyses were performed using R version 3.6.2 (R Core Team, 2019).

3. Results

3.1 Transformation of inorganic to organic carbon by microbial fixation

Subsequent to *in situ* tracing, the ^{13}C-SOC content in the bulk soil at sampling plots was detected (Figure 2). The mean ^{13}C-SOC content in the bulk soil was 6.881 mg m^{-2} during the feeding periods and showed dramatically variation, from 1.047 to 17.433 mg m^{-2} at the plots (Figure 2). After the feeding protocol, CO_2 content in the feeding chambers was 1240.487 μmol mol^{-1} (1152.421 μmol mol^{-1} of $^{12}CO_2$ and 88.225 μmol mol^{-1} of $^{13}CO_2$), and CO_2 content in the soil was 1391.611 μmol mol^{-1} (1297.629 μmol mol^{-1} of $^{12}CO_2$ and 93.983 μmol mol^{-1} of $^{13}CO_2$) (Table 1). On the basis of

differences in $^{13}CO_2$ content in the feeding chambers before and after the tracing protocol, the total amount of ^{13}C absorbed by the soil was determined to be 37.443 mg (3.973 mg kg^{-1} in soil).

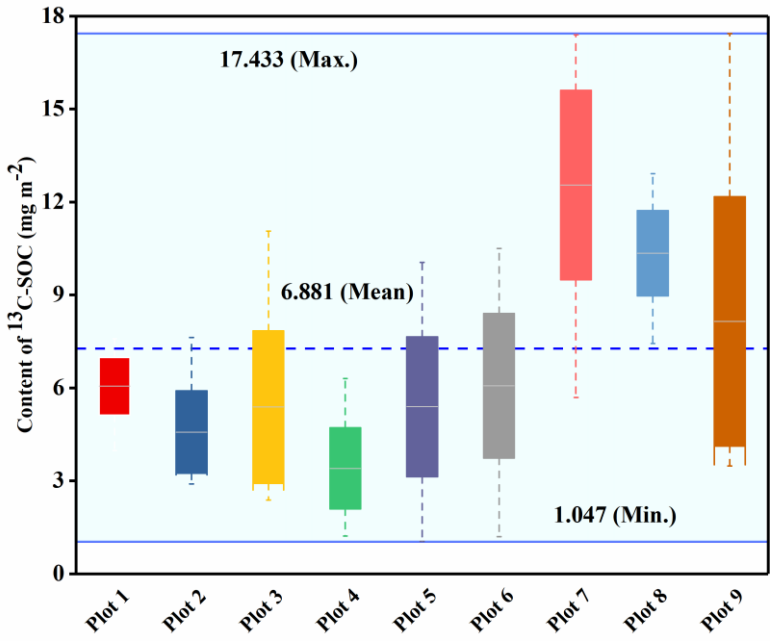

Figure 2. Contents of the microbial carbon transformed from inorganic carbon to organic carbon (^{13}C-SOC) among the sampling plots during the feeding periods.

Table 1 Contents and components of CO_2 in the feeding chambers and soil after feeding protocols (mean ± SD)

	CO_2 (μmol mol^{-1})	$^{12}CO_2$ (μmol mol^{-1})	$^{13}CO_2$ (μmol mol^{-1})
Chambers	1240.487 ± 320.005	1152.421 ± 318.331	88.225 ± 21.379
Soil collars	1391.611 ± 380.447	1297.629 ± 377.928	93.983 ± 11.766

3.2 Functional and taxonomic characterization of soil microbes associated with inorganic carbon transformation

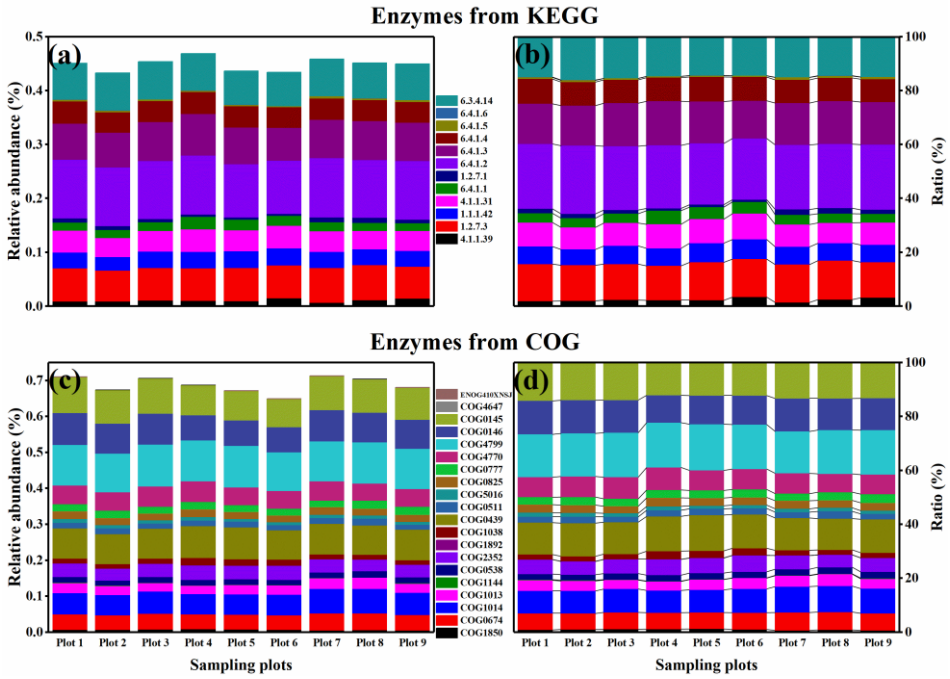

Figure 3. Relative abundance (a, c) and ratios (b, d) of identified genes encoding enzymes (EC in KEGG and COG in eggNOG are given) related to microbial fixation at the sampling plots.

Metagenomic analysis identified genes encoding enzymes related to microbial CO_2 and HCO_3^- fixation, which represented 0.448% (KEGG) and 0.668% (eggNOG) of all ascertained genes (Figure 3). The relative abundance of the genes related to HCO_3^- transformation was higher than the genes associated with CO_2 transformation. Of those, genes encoding enzymes of the ribulose-bisphosphate carboxylase, 2-oxoglutarate synthase, isocitrate dehydrogenase ($NADP^+$), phosphoenolpyruvate carboxylase, pyruvate carboxylase, pyruvate synthase, acetyl-CoA carboxylase, and propionyl-CoA carboxylase were detected in the sampling plots (Figure 3). These enzymes are mainly employed for autotrophic carbon fixation, by which soil CO_2 and HCO_3^- are converted to SOC. The relative abundance of these genes was 0.339%

285 (KEGG) and 0.518% (eggNOG) of all identified genes, accounting for 75.644%
286 (KEGG) and 75.298% (eggNOG) of all detected genes for microbial inorganic carbon
287 transformation.

288 Additionally, the genes encoding enzymes that contribute to the biosynthesis of
289 fatty acids and anaplerotic reactions such as methylcrotonoyl-CoA carboxylases,
290 geranoyl-CoA carboxylase, phosphoenolpyruvate carboxykinase, acetone
291 carboxylases, and biotin carboxylases were also found based on KEGG and eggNOG
292 analyses (Figure 3). The presence of such genes suggests the role of heterotrophic
293 pathways for inorganic carbon transformation. As shown in Figure 4, soil microbes
294 encoding enzymes involved in inorganic carbon transformation, such as ribulose-
295 bisphosphate carboxylase (0.030%; total relative abundance of the detected
296 microbes), 2-oxoglutarate synthase (0.180%), isocitrate dehydrogenase ($NADP^+$)
297 (0.180%), phosphoenolpyruvate carboxylase (0.185%), pyruvate carboxylase
298 (0.080%), pyruvate synthase (0.032%), acetyl-CoA carboxylase (0.255%), propionyl-
299 CoA carboxylase (0.098%), methylcrotonoyl-CoA carboxylase (0.033%), and
300 geranoyl-CoA carboxylase (0.003%), were determined in the sampling plots. These
301 microbes mainly belonged to the phyla Actinobacteria, Proteobacteria, Chloroflexi,
302 Acidobacteria, Gemmatimonadetes, Microgenomates, and Nitrospirae (Figure 4). The
303 microbial composition and relative abundance varied depending upon the kind of
304 enzyme.

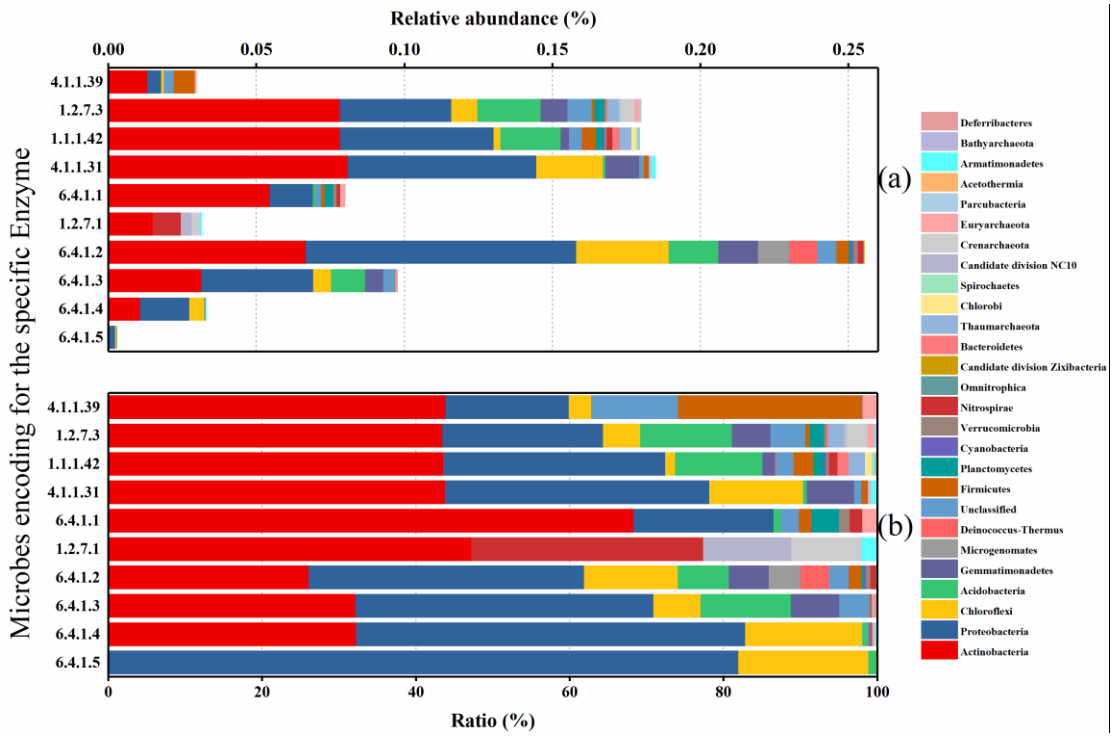

Figure 4. Relative abundance (a) and ratios (b) of microbes encoding enzymes (Enzyme Commission numbers (EC) in KEGG are given) at the sampling plots.

3.3 Correlation between ^{13}C-SOC and bicarbonate, CO_2, $^{13}CO_2$, and $^{12}CO_2$ content in addition to microbes.

The ^{13}C-SOC content significantly correlated with bicarbonate, CO_2, and $^{12}CO_2$ content in the soil ($P < 0.05$), and did not correlate with the $^{13}CO_2$ content ($P > 0.05$, Figure 5). Additionally, the content of ^{13}C-SOC remarkably correlated with genes involved in CO_2 transformation, based on KEGG ($P = 0.044$) and COG ($P = 0.047$) database prediction, whereas it lacked correlation with the gene components involved in HCO_3^- transformation ($P > 0.05$) (Table 2). Of all the identified genes, the content of ^{13}C-SOC significantly correlated with the relative abundance of genes encoding

enzymes such as 2-oxoglutarate synthase, pyruvate synthase, and geranoyl-CoA carboxylase, based on KEGG database; and genes encoding ribulose-bisphosphate carboxylase, 2-oxoglutarate synthase, and isocitrate dehydrogenase (NADP+) based on eggNOG database (Table 3).

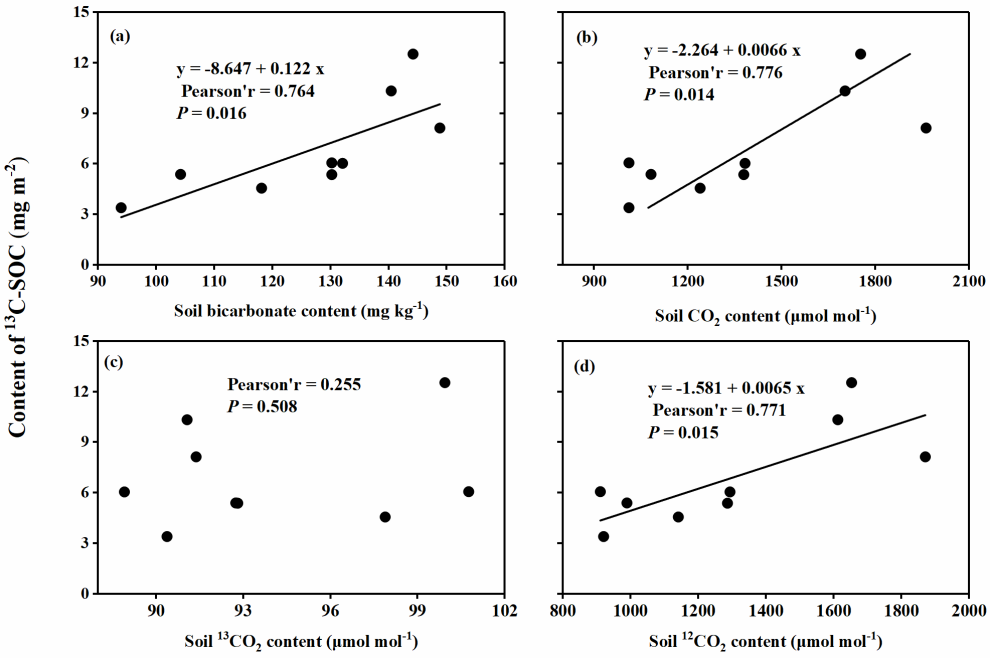

Figure 5. Correlation between ^{13}C-SOC content and bicarbonate (a), CO_2 (b), $^{13}CO_2$ (c), and $^{12}CO_2$ content (d) in soil.

As determined by Mantel test, significant correlation was observed between the ^{13}C-SOC content and microorganisms harboring acetyl-CoA carboxylase, propionyl-CoA carboxylase, and methylcrotonoyl-CoA carboxylase ($P < 0.05$; Table 4). Moreover, ^{13}C-SOC content marginally correlated with microorganism harboring ribulose-bisphosphate carboxylase, 2-oxoglutarate synthase, and isocitrate dehydrogenase (NADP+) ($0.05 < P < 0.10$; Table 4). Further analysis revealed

334 significant correlation between ^{13}C-SOC content and PC scores of microbes encoding
335 carrying the six above-mentioned enzymes ($P < 0.05$; Figure 6).

336

337 **Table 2** Correlation between gene components and ^{13}C-SOC content as determined by Mantel
338 test

Functional category of genes	Database	*r*	*P*
All genes associated with carbon transformation	KEGG	-0.076	0.667
	COG	0.231	0.095
Genes associated with CO_2 transformation	KEGG	**0.290**	**0.044**
	COG	**0.290**	**0.047**
Genes associated with HCO_3^- transformation	KEGG	-0.162	0.695
	COG	-0.033	0.524

339

340 **Table 3** Correlation between the relative abundance of gene components and ^{13}C-SOC
341 content

KEGG numbers	*t*	*r*	*P*	COG numbers	*t*	*r*	*P*
4.1.1.39	-0.524	-0.159	0.684	COG1850	**-3.586**	**-0.805**	**0.009**
1.2.7.3	**2.830**	**0.730**	**0.025**	COG0674	**3.767**	**0.818**	**0.007**
1.1.1.42	0.118	0.045	0.909	COG1014	**7.229**	**0.939**	**<0.001**
4.1.1.31	-1.282	-0.435	0.241	COG1013	**3.499**	**0.798**	**0.010**
6.4.1.1	-1.348	-0.454	0.220	COG1144	-0.391	-0.146	0.707
1.2.7.1	**2.986**	**0.748**	**0.020**	COG0538	**2.472**	**0.683**	**0.043**
6.4.1.2	0.581	0.214	0.580	COG2352	-1.246	-0.426	0.253
6.4.1.3	0.340	0.127	0.744	COG1892	-1.275	-0.434	0.243
6.4.1.4	-0.553	-0.204	0.598	COG1038	-1.579	-0.512	0.158
6.4.1.5	**4.623**	**0.868**	**0.002**	COG0439	-0.808	-0.292	0.446
6.4.1.6	0.167	0.063	0.872	COG0511	0.864	0.310	0.416
6.3.4.14	-0.061	-0.023	0.953	COG5016	-0.414	-0.155	0.691

	COG0825	0.240	0.091	0.817
	COG0777	0.284	0.107	0.785
	COG4770	-0.990	-0.350	0.355
	COG4799	-0.136	-0.051	0.896
	COG0146	1.482	0.489	0.182
	COG0145	0.814	0.294	0.442
	COG4647	0.211	0.080	0.839
	ENOG410XNSJ	0.618	0.227	0.556

Bold numbers indicate statistical significance at $P < 0.05$.

Table 4 Correlation between the community compositions of microbes encoding enzymes and ^{13}C-SOC content as determined by the Mantel test

Encoded enzyme	*r*	*P*
Ribulose-bisphosphate carboxylase (4.1.1.39)	**0.294**	**0.062**
2-oxoglutarate synthase (1.2.7.3)	**0.398**	**0.066**
Isocitrate dehydrogenase (NADP+) (1.1.1.42)	**0.255**	**0.095**
Phosphoenolpyruvate carboxylase (4.1.1.31)	0.185	0.221
Pyruvate carboxylase (6.4.1.1)	0.123	0.201
Pyruvate synthase (1.2.7.1)	0.032	0.370
Acetyl-CoA carboxylase (6.4.1.2)	**0.400**	**0.015**
Propionyl-CoA carboxylase (6.4.1.3)	**0.301**	**0.048**
Methylcrotonoyl-CoA carboxylase (6.4.1.4)	**0.698**	**0.003**
Geranoyl-CoA carboxylase (6.4.1.5)	0.100	0.332

Numbers in brackets refer to Enzyme Commission numbers of the KEGG database. Bold numbers indicate statistical significance and marginal significance at $P < 0.05$ and $0.05 < P < 0.10$.

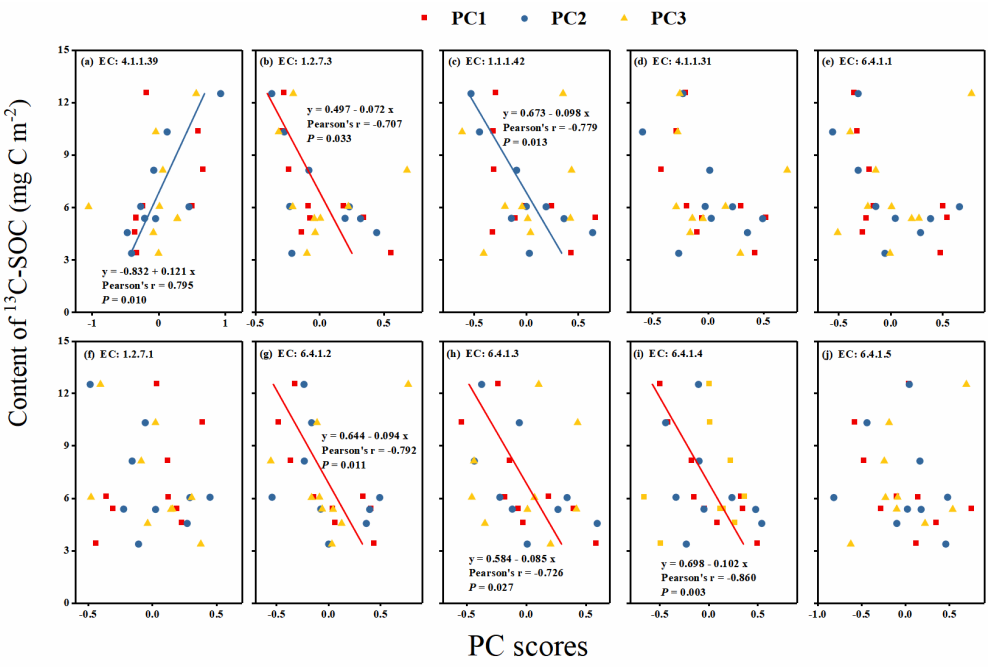

Figure 6. Correlation analysis of principal component scores of microbes encoding carbon fixation enzymes (numbers refer to Enzyme Commission numbers) and ^{13}C-SOC content.

4. Discussion

As anticipated, our results showed that the signature profile of ^{13}C in SOC originated from $^{13}CO_2$ in the desert soil (Figure 2). In the tracing experiment, a large portion of $^{13}CO_2$ in the chamber was absorbed into the soil (Table 1) and was converted mainly to soil $^{13}CO_2$ and $H^{13}CO_3^-$ (Fa et al., 2016a), suggesting that a part of SIC was positively labeled and further participated in the process of microbial transformation from inorganic (CO_2 and HCO_3^-) to organic carbon. Additionally, metagenomics of sample material predicted the microbes poses genetic potential to incorporate CO_2 and HCO_3^- present in the desert soil (Figure 3 and Figure 4); microbial metabolic pathways correlated with ^{13}C-SOC content (Table 2, 3, and 4;

Figure 6). Taken together, these results confirmed that SIC, including soil CO_2 and HCO_3^-, was transformed into SOC via microbial metabolism.

Our results showed that *in vivo* CO_2 exchange between the chamber and collar, and atmosphere and soil, occurred during the tracing protocols. Approximately four fifths of $^{13}CO_2$ was introduced into the desert soil (Table 1) and converted to soil CO_2 and HCO_3^-. The $^{13}CO_2$ content in the soil collars occupied 7.112% of the total CO_2 (Table 1). Although no test of $^{13}C/^{12}C$ in HCO_3^- was conducted, a large portion of introduced $^{13}CO_2$ is stored in the form of HCO_3^- according to previous studies in these regions (Fa et al., 2016a, 2016b; Wang et al., 2019). In addition, the significant relationship between ^{13}C-SOC content and soil CO_2 and bicarbonate content (Figure 5) demonstrated that the microbial transformation processes were possibly associated with these two forms of inorganic carbon. However, no remarkable correlation was detected with respect to the soil $^{13}CO_2$ content (Table 1), which may be the result of the relatively low content of soil $^{13}CO_2$, along with the intense abiotic conversion processes ($CO_2 + H_2O \leftrightarrow H^+ + HCO_3^- \leftrightarrow CO_3^{2-} + 2H^+$). Nevertheless, these labeled soil CO_2 and HCO_3^- can serve as the carbon source for such microbial transformation in the desert soil.

As for carbon sources, both soil CO_2 and HCO_3^- is assimilated by microbes and transformed into SOC, which was supported by the functional and taxonomic characterization of soil microbes involved in fixation associated with carbon transformation (Figure 3 and Figure 4), and the linkage between ^{13}C-SOC and associated putative genes (Table 2, Table 3, Table 4, Figure 5, and Figure 6).

386 According to the prediction of microbial fixation enzymes, microbes with operating
387 autotrophic and heterotrophic pathways were found in the desert soil (Figure 3).
388 Specifically, microbes harboring these genes mainly contributed toward autotrophic
389 fixation, including rTCA cycle, 3-HP and 3-HP/4-HB cycles, and DC/4-HB cycle; in
390 addition, a few genes contributed to the Calvin cycle, followed by heterotrophic
391 fixation (Figure 3; Figure 4; Table S1; Berg 2011). Microbes harboring similar genes
392 have been found in the desert soil (Liu et al., 2018; Zhao et al., 2018), and many other
393 surroundings, e.g., paddy soils, grasslands, wetlands, carbonate cave, Precambrian
394 continental crust, and subsurface fracture fluids (Ge et al., 2016; Long et al., 2015;
395 Magnabosco et al., 2016; Momper et al., 2017; Nowak et al., 2015; Ortiz et al., 2014).
396 Our results were different from prior studies with incubation experiments showing
397 that the Calvin cycle is responsible for microbial carbon fixation in drylands (Lynn et
398 al., 2017; Zhao et al., 2018). The phototrophic process is probably inhibited because
399 of the combined effects of water deficit and intense UV radiation (Bay et al. 2018).
400 Furthermore, several studies have also demonstrated that phototrophs are not present
401 in Atacama Desert soil (Costello et al. 2009), and the microbial carbon fixation in the
402 dark is speculated to be the origin of energy and organic carbon sources in the soil
403 (Lynch et al. 2012 and 2014; Zhao et al., 2018). Moreover, Zhao et al. (2018)
404 investigated the CO_2 fixation capacity of the autotrophic microbial community via the
405 Calvin cycle in desert and steppe soils; however, the result indicates that alternative
406 carbon fixation pathways account for a portion of the carbon fixation. As discussed
407 above, we conclude that desert soil microbes mainly employ dark microbial fixation

pathways (chemoautotrophic and heterotrophic pathways) for SIC transformation into SOC.

In particular, our results show that a considerable portion of the determined genes and associated taxa were responsible for heterotrophic CO_2 fixation in the desert soil (Figure 3 and 4) and significantly correlated with ^{13}C-SOC content (Table 4 and Figure 6), implying that the existing heterotrophic processes also play an important role in inorganic carbon transformation in desert soil. This finding extended the available knowledge of microbial carbon fixation processes in desert soils (Liu et al., 2018; Lynn et al., 2017; Zhao et al., 2018). Heterotrophs incorporate inorganic carbon using a variety of carboxylation reactions that are part of the core or peripheral metabolic pathways (Šantrůčková et al., 2018). In nutrient-limited desert soils, the importance of this pathway increases because microbes experience carbon limitation on account of the disproportion between carbon demand for energy generation and growth, and its availability (Alonso-Sáez et al., 2010). Thereby, they increasingly rely on anaplerotic fixation and *de novo* amino acid synthesis (Nel & Cramer, 2019). Given that existing studies have determined dark microbial fixation processes via stable carbon tracing methods and/or stable-isotope probing (Nel & Cramer, 2019; Šantrůčková et al. 2018), the metagenomic analysis strongly enhance the certainty of heterotrophic fixation processes in the soil. Despite the contribution of heterotrophic processes to the total microbial fixation, it cannot be determined solely based on genetic potential. Nevertheless, our results suggest that the desert soil indeed contains microbes with genetic potential for heterotrophic fixation.

In the present study, different microbial metabolic processes were predicted based on the KEGG and eggNOG databases (Figure 3 and Table 3); the overall trends reflected were the same, i.e., the soil CO_2 and HCO_3^- can be transformed to SOC by desert soil microbes. Further, our results demonstrated that the relative abundance of the genes related to HCO_3^- transformation was higher than the genes related to CO_2 transformation (Figure 3), and the different relationships between these two genes and ^{13}C-SOC (Table 2 and 3), indicating that the microbial processes related to CO_2 metabolism is more efficient than that of HCO_3^- metabolism, in case of SIC transformation to SOC.

Based on the isotopic tracing method and the metagenomic prediction, the carbon transformation process from SIC into SOC through dark microbial fixation was determined in this study. According to the ratio of ^{13}C to ^{12}C in the soil CO_2 (Table 1) and HCO_3^-, together with the content of labeled SIC (approximately 3.973 mg kg^{-1} in soil) after tracing protocols, we estimate that the actual intensity of microbial carbon transformation in the desert soil may be more than 10 times of the intensity obtained by the tracing method (if do not consider the isotopic fractionation effect of microbial conversion). As dead microbial biomass (microbial necromass) is relatively stable in soil compared to plant detritus (Liang et al., 2017), the organic carbon produced through the dark microbial fixation likely remains much longer in the soil compared to the organic carbon that enters the soil from plant detritus. Thus, microbial biomass might substantially contribute to the formation of organic matter in the desert soil (Spohn et al., 2020). This portion of organic matter is of particular importance in the

context of low primary production and harsh environment of drylands, as it can contribute to fertility and nutrient supply for biogeochemical cycles in deserts. Moreover, recent studies show that the SIC pool in drylands is not stable as previously estimated (An et al., 2019; Wang et al., 2013; Zamanian et al., 2016) and is probably affected by changes in land utilization, acid deposition, and nitrogen fertilization (An et al., 2019; Yang et al., 2012; Zamanian et al., 2019). These factors give rise to variations and decreased stability of SIC composition, demonstrating that carbon is transformed from carbonates into forms of CO_2 and/or HCO_3^-. Due to the increment of soil CO_2 and HCO_3^-, the dark microbial fixation process in drylands tends to be enhanced (Figure 5), and therefore may offset the soil CO_2 emission from soils of drylands and maintain the function of soil carbon sequestration.

Complete evaluation of dark microbial fixation processes, in terms of the long-term quantity and stability of SOC production, with the help of a mathematical model is essential to clearly investigate the contribution of dark microbial fixation for formation of soil organic matter. Overall, our work provides field-based empirical evidence illustrating SIC (soil CO_2 and HCO_3^-) transformation into SOC via the dark microbial fixation pathway in desert soil. This study delineated the process of transformation of different soil carbon pools and the potential function of the inorganic carbon in drylands.

5. Conclusions

On the basis of *in situ* tracing of soil inorganic carbon in bulk soil and predicting the associated microbial metabolic processes on the basis of functional and taxonomic characterization by metagenomic analysis, we demonstrate that soil inorganic carbon can be transformed into organic carbon through dark microbial fixation in the desert. Although we cannot fully ascertain the portion of SOC in the soil derived from dark microbial fixation, the present study suggests an inorganic to organic carbon transformation driven by microbe-mediated metabolic pathways. We highlight a neglected carbon transformation process in soil pools and broadening the knowledge of the potential function of soil inorganic carbon in drylands.

Acknowledgments, Samples, and Data

We would like to thank the staff of the Yanchi Research Station for their assistance with field and laboratory work. We are also grateful to the anonymous reviewers for their constructive and valuable comments and suggestions that helped us improve this. This work was supported by the National Natural Science Foundation of China [NFSC, grant number 31670709]; the National Key Research and Development Program of China [grant number 2016YFC0500905]; the Fundamental Research Funds for the Central Universities [grant number 2015ZCQ-SB-02]; and a project funded by the China Postdoctoral Science Foundation [grant number 2016M600938]. Metagenomics data were submitted to NCBI under biosample accession number SAMN08366930. The authors declare no conflicts of interest. Data for this manuscript are available at Figshare (https://figshare.com/s/2f8b42d016e8e1d6db69).

References

Alonso-Sáez, L., Galand, P. E., Casamayor, E. O., Pedros-Alio, C., & Bertilsson, S. (2010). High bicarbonate assimilation in the dark by Arctic bacteria. *The ISME journal*, *4*(12), 1581-1590. https://doi.org/10.1038/ismej.2010.69

An, H., Wu, X., Zhang, Y., & Tang, Z. (2019). Effects of land-use change on soil inorganic carbon: A meta-analysis. *Geoderma*, *353*, 273-282. https://doi.org/10.1016/j.geoderma.2019.07.008

Bar-Even, A., Noor, E., & Milo, R. (2012). A survey of carbon fixation pathways through a quantitative lens. *Journal of experimental botany*, *63*(6), 2325-2342. https://doi.org/10.1093/jxb/err417

Bay, S., Ferrari, B., & Greening, C. (2018). Life without water: how do bacteria generate biomass in desert ecosystems. *Microbiology Australia*, *39*, 28-32. https://doi.org/10.1071/MA18008

Berg, I. A. (2011). Ecological aspects of the distribution of different autotrophic CO_2 fixation pathways. *Applied and environmental microbiology*, *77*(6), 1925-1936. https://doi.org/10.1128/AEM.02473-10

Beulig, F., Urich, T., Nowak, M., Trumbore, S. E., Gleixner, G., Gilfillan, G. D., Fjelland, K. E., & Küsel, K. (2016). Altered carbon turnover processes and microbiomes in soils under long-term extremely high CO_2 exposure. *Nature microbiology*, *1*(2), 1-10. https://doi.org/10.1038/nmicrobiol.2015.25

516 Costello, E. K., Halloy, S. R., Reed, S. C., Sowell, P., & Schmidt, S. K. (2009).
517 Fumarole-supported islands of biodiversity within a hyperarid, high-elevation
518 landscape on Socompa Volcano, Puna de Atacama, Andes. *Applied and*
519 *Environmental Microbiology*, *75*(3), 735-747. https://doi.org/10.1128/AEM.01469-08
520 Emmerich, W. E. (2003). Carbon dioxide fluxes in a semiarid environment with high
521 carbonate soils. *Agricultural and Forest Meteorology*, *116*(1-2), 91-102.
522 https://doi.org/10.1016/S0168-1923(02)00231-9
523 Fa, K. Y., Zhang, Y. Q., Wu, B., Qin, S. G., Liu, Z., & She, W. W. (2016b). Patterns
524 and possible mechanisms of soil CO_2 uptake in sandy soil. *Science of the Total*
525 *Environment*, *544*, 587-594. https://doi.org/10.1016/j.scitotenv.2015.11.163
526 Fa, K., Liu, Z., Zhang, Y., Qin, S., Wu, B., & Liu, J. (2016a). Abiotic carbonate
527 dissolution traps carbon in a semiarid desert. *Scientific reports*, *6*, 23570.
528 https://doi.org/10.1038/srep23570
529 Gago, G., Diacovich, L., Arabolaza, A., Tsai, S. C., & Gramajo, H. (2011). Fatty acid
530 biosynthesis in actinomycetes. FEMS microbiology reviews, 35(3), 475-497.
531 https://doi.org/10.1111/j.1574-6976.2010.00259.x
532 Gao, Y., Dang, P., Zhao, Q., Liu, J., & Liu, J. (2018). Effects of vegetation
533 rehabilitation on soil organic and inorganic carbon stocks in the Mu Us Desert,
534 northwest China. *Land Degradation & Development*, *29*(4), 1031-1040.
535 https://doi.org/10.1002/ldr.2832

Ge, T., Wu, X., Liu, Q., Zhu, Z., Yuan, H., Wang, W., Whiteley, A. S., & Wu, J. (2016). Effect of simulated tillage on microbial autotrophic CO_2 fixation in paddy and upland soils. *Scientific reports*, *6*, 19784. https://doi.org/10.1038/srep19784

Hügler, M., & Sievert, S. M. (2011). Beyond the Calvin cycle: autotrophic carbon fixation in the ocean. *Annual review of marine science*, *3*, 261-289. https://doi.org/10.1146/annurev-marine-120709-142712

Jia, X., Zha, T., Gong, J., Zhang, Y., Wu, B., Qin, S., & Peltola, H. (2018). Multi-scale dynamics and environmental controls on net ecosystem CO_2 exchange over a temperate semiarid shrubland. *Agricultural and Forest Meteorology*, *259*, 250-259. https://doi.org/10.1016/j.agrformet.2018.05.009

Kanehisa, M., Goto, S., Kawashima, S., Okuno, Y., & Hattori, M. (2004). The KEGG resource for deciphering the genome. *Nucleic acids research*, *32*(suppl_1), D277-D280. https://doi.org/10.1093/nar/gkh063

Lal, R. (2009). Sequestering carbon in soils of arid ecosystems. *Land Degradation & Development*, *20*(4), 441-454. https://doi.org/10.1002/ldr.934

Liang, C., Schimel, J. P., & Jastrow, J. D. (2017). The importance of anabolism in microbial control over soil carbon storage. *Nature microbiology*, *2*(8), 1-6. https://doi.org/10.1038/nmicrobiol.2017.105

Liu, J., Fa, K., Zhang, Y., Wu, B., Qin, S., & Jia, X. (2015). Abiotic CO_2 uptake from the atmosphere by semiarid desert soil and its partitioning into soil phases. *Geophysical Research Letters*, *42*(14), 5779-5785. https://doi.org/10.1002/2015GL064689

Liu, Z., Sun, Y., Zhang, Y., Feng, W., Lai, Z., Fa, K., & Qin, S. (2018). Metagenomic and 13C tracing evidence for autotrophic atmospheric carbon absorption in a semiarid desert. *Soil Biology and Biochemistry*, *125*, 156-166. https://doi.org/10.1016/j.soilbio.2018.07.012

Liu, Z., Sun, Y., Zhang, Y., Qin, S., Sun, Y., Mao, H., & Miao, L. (2020). Desert soil sequesters atmospheric CO_2 by microbial mineral formation. *Geoderma*, *361*, 114104. https://doi.org/10.1016/j.geoderma.2019.114104

Long, X. E., Yao, H., Wang, J., Huang, Y., Singh, B. K., & Zhu, Y. G. (2015). Community structure and soil pH determine chemoautotrophic carbon dioxide fixation in drained paddy soils. *Environmental Science & Technology*, *49*(12), 7152-7160. https://doi.org/10.1021/acs.est.5b00506

Lynch, R. C., Darcy, J. L., Kane, N. C., Nemergut, D. R., & Schmidt, S. K. (2014). Metagenomic evidence for metabolism of trace atmospheric gases by high-elevation desert *Actinobacteria*. *Frontiers in microbiology*, *5*, 698. https://doi.org/10.3389/fmicb.2014.00698

Lynch, R. C., King, A. J., Farías, M. E., Sowell, P., Vitry, C., & Schmidt, S. K. (2012). The potential for microbial life in the highest-elevation (> 6000 m.a.s.l.) mineral soils of the Atacama region. *Journal of Geophysical Research: Biogeosciences*, *117*(G2). https://doi.org/10.1029/2012JG001961

Lynn, T. M., Ge, T., Yuan, H., Wei, X., Wu, X., Xiao, K., Kumaresan D., Yu, S. S., Wu, J., & Whiteley, A. S. (2017). Soil carbon-fixation rates and associated bacterial

579 diversity and abundance in three natural ecosystems. *Microbial ecology*, *73*(3), 645-
580 657. https://doi.org/10.1007/s00248-016-0890-x
581 Magnabosco, C., Ryan, K., Lau, M. C., Kuloyo, O., Lollar, B. S., Kieft, T. L., van
582 Heerden, E., & Onstott, T. C. (2016). A metagenomic window into carbon
583 metabolism at 3 km depth in Precambrian continental crust. *The ISME journal*, *10*(3),
584 730-741. https://doi.org/10.1038/ismej.2015.150
585 Miltner, A., Kopinke, F. D., Kindler, R., Selesi, D., Hartmann, A., & Kästner, M.
586 (2005). Non-phototrophic CO_2 fixation by soil microorganisms. *Plant and*
587 *Soil*, *269*(1-2), 193-203. https://doi.org/10.1007/s11104-004-0483-1
588 Miltner, A., Richnow, H. H., Kopinke, F. D., & Kästner, M. (2004). Assimilation of
589 CO_2 by soil microorganisms and transformation into soil organic matter. *Organic*
590 *Geochemistry*, *35*(9), 1015-1024. https://doi.org/10.1016/j.orggeochem.2004.05.001
591 Momper, L., Jungbluth, S. P., Lee, M. D., & Amend, J. P. (2017). Energy and carbon
592 metabolisms in a deep terrestrial subsurface fluid microbial community. *The ISME*
593 *journal*, *11*(10), 2319-2333. https://doi.org/10.1038/ismej.2017.94
594 Monger, H. C., Kraimer, R. A., Khresat, S. E., Cole, D. R., Wang, X., & Wang, J.
595 (2015). Sequestration of inorganic carbon in soil and groundwater. *Geology*, *43*(5),
596 375-378. https://doi.org/10.1130/G36449.1
597 Nel, J. A., & Cramer, M. D. (2019). Soil microbial anaplerotic CO_2 fixation in
598 temperate soils. *Geoderma*, *335*, 170-178.
599 https://doi.org/10.1016/j.geoderma.2018.08.014

Nowak, M., Beulig, F., von Fischer, J., Muhr, J., Küsel, K., & Trumbore, S. E. (2015). Autotrophic fixation of geogenic CO_2 by microorganisms contributes to soil organic matter formation and alters isotope signatures in a wetland mofette. *Biogeosciences*, *12*(3), 7169-7183. https://doi.org/10.5194/bg-12-7169-2015.

Ortiz, M., Legatzki, A., Neilson, J. W., Fryslie, B., Nelson, W. M., Wing, R. A., Soderlund, C. A., Pryor, B. M., & Maier, R. M. (2014). Making a living while starving in the dark: metagenomic insights into the energy dynamics of a carbonate cave. *The ISME journal*, *8*(2), 478-491. https://doi.org/10.1038/ismej.2013.159

R Core Team (2019). R: A Language and Environment for Statistical Computing. Vienna: R Foundation for Statistical Computing.

Reynolds, J. F., Smith, D. M. S., Lambin, E. F., Turner, B. L., Mortimore, M., Batterbury, S. P. J., Downing, T. E., Dowlatabadi, H., Fernández, R. J., Herrick, J. E., Huber-Sannwald, E., Jiang, H., Leemans, R., Lynam, T., Maestre, F. T., Ayarza, M., & Walker, M. (2007). Global desertification: building a science for dryland development. *science*, *316*(5826), 847-851. https://doi.org/10.1126/science.1131634

Safriel, U., & Adeel, Z. (2005). Dryland systems. In Hassan, R., Scholes, R., & Ash, N., (Eds.), *Ecosystems and Human Well-Being*, *Current State and Trends* (pp. 625–658). Washington, DC: Island Press.

Šantrůčková, H., Kotas, P., Bárta, J., Urich, T., Čapek, P., Palmtag, J., Alves, R. J. E., Biasi, C., Diáková, K., Gentsch, N., Gittel, A., Guggenberger, G., Hugelius, G., Lashchinsky, N., Martikainen, P. J., Mikuttai, R., Schleper, C., Schnecker, J., Schwab, C., Shibistova, O., Wildk, B., & Gittel, A. (2018). Significance of dark CO_2 fixation

622 in arctic soils. *Soil Biology and Biochemistry*, *119*, 11-21.
623 https://doi.org/10.1016/j.soilbio.2017.12.021
624 Schühle, K., & Heider, J. (2012). Acetone and butanone metabolism of the
625 denitrifying bacterium "*Aromatoleum aromaticum*" demonstrates novel biochemical
626 properties of an ATP-dependent aliphatic ketone carboxylase. *Journal of*
627 *bacteriology*, *194*(1), 131-141. https://doi.org/10.1128/JB.05895-11
628 Shi, Y., Baumann, F., Ma, Y., Song, C., Kühn, P., Scholten, T., & He, J. S. (2012).
629 Organic and inorganic carbon in the topsoil of the Mongolian and Tibetan grasslands:
630 pattern, control and implications. *Biogeosciences*, *9*(6), 2287.
631 https://doi.org/10.5194/bg-9-2287-2012
632 Spohn, M., Müller, K., Höschen, C., Mueller, C. W., & Marhan, S. (2020). Dark
633 microbial CO_2 fixation in temperate forest soils increases with CO_2
634 concentration. *Global Change Biology*, *26*(3), 1926-1935.
635 https://doi.org/10.1111/gcb.14937
636 Steinbeiss, S., Temperton, V. M., & Gleixner, G. (2008). Mechanisms of short-term
637 soil carbon storage in experimental grasslands. *Soil Biology and Biochemistry*, *40*(10),
638 2634-2642. https://doi.org/10.1016/j.soilbio.2008.07.007
639 Tong, L. (2013). Structure and function of biotin-dependent carboxylases. *Cellular*
640 *and Molecular Life Sciences*, *70*(5), 863-891. https://doi.org/10.1007/s00018-012-
641 1096-0

642 Tran, T. H., Hsiao, Y. S., Jo, J., Chou, C. Y., Dietrich, L. E., Walz, T., & Tong, L.
643 (2015). Structure and function of a single-chain, multi-domain long-chain acyl-CoA
644 carboxylase. *Nature*, *518*(7537), 120-124. https://doi.org/10.1038/nature13912
645 Walkley, A., & Black, I. A. (1934). An examination of the Degtjareff method for
646 determining soil organic matter, and a proposed modification of the chromic acid
647 titration method. *Soil science*, *37*(1), 29-38.
648 Wang, J. P., Wang, X. J., Zhang, J., & Zhao, C. Y. (2015). Soil organic and inorganic
649 carbon and stable carbon isotopes in the Yanqi Basin of northwestern
650 China. *European Journal of Soil Science*, *66*(1), 95-103. https://doi.
651 org/10.1111/ejss.12188
652 Wang, J., Zhang, F., Kung, H. T., Ren, Y., Zhang, Y., & Yu, H. (2017). Linkage
653 analysis of land use/cover patterns and hydro-chemical characteristics in different
654 seasons in ebinur lake watershed, China. *Water*, *9*(11), 888.
655 https://doi.org/10.3390/w9110888
656 Wang, X., Jiang, Z., Li, Y., Kong, F., & Xi, M. (2019). Inorganic carbon
657 sequestration and its mechanism of coastal saline-alkali wetlands in Jiaozhou Bay,
658 China. *Geoderma*, *351*, 221-234. https://doi.org/10.1016/j.geoderma.2019.05.027
659 Wang, Y., Wang, Z., & Li, Y. (2013). Storage/turnover rate of inorganic carbon and
660 its dissolvable part in the profile of saline/alkaline soils. *PloS One*, *8*(11), e82029.
661 https://doi.org/10.1371/journal.pone.0082029
662 Yang, Y., Fang, J., Ji, C., Ma, W., Mohammat, A., Wang, S., Wang, P., Datta, A.,
663 Robinson, D., & Smith, P. (2012). Widespread decreases in topsoil inorganic carbon

664 stocks across China's grasslands during 1980s–2000s. *Global Change*
665 *Biology*, *18*(12), 3672-3680.
666 Zamanian, K., & Kuzyakov, Y. (2019). Contribution of soil inorganic carbon to
667 atmospheric CO_2: More important than previously thought. *Global change*
668 *biology*, *25*(1), e1-e3. https://doi.org/10.1111/gcb.14463
669 Zamanian, K., Pustovoytov, K., & Kuzyakov, Y. (2016). Pedogenic carbonates:
670 Forms and formation processes. *Earth-Science Reviews*, *157*, 1-17.
671 https://doi.org/10.1016/j.earscirev.2016.03.003
672 Zamanian, K., Zarebanadkouki, M., & Kuzyakov, Y. (2018). Nitrogen fertilization
673 raises CO_2 efflux from inorganic carbon: A global assessment. *Global Change*
674 *Biology*, *24*(7), 2810-2817. https://doi.org/10.1111/gcb.14148
675 Zhao, K., Kong, W., Wang, F., Long, X. E., Guo, C., Yue, L., Yao, H., & Dong, X.
676 (2018). Desert and steppe soils exhibit lower autotrophic microbial abundance but
677 higher atmospheric CO_2 fixation capacity than meadow soils. *Soil Biology and*
678 *Biochemistry*, *127*, 230-238. https://doi.org/10.1016/j.soilbio.2018.09.034